

Effect of Product Microstructure and Process Parameters on Modified Atmosphere Packaged Bread

Sofie Morren¹  · Quang Tri Ho² · Jesse Stoops¹ · Tim Van Dyck¹ · Johan Claes¹ · Pieter Verboven² · Bart Nicolai² · Leen Van Campenhout¹

Received: 5 June 2015 / Accepted: 24 October 2016 / Published online: 5 November 2016
© Springer Science+Business Media New York 2016

Abstract The objective of this study was to examine bread microstructure, oxygen diffusion properties, and gas exchange between bread and headspace after packaging in modified atmosphere (MA). Breads were produced at laboratory scale, and industrially produced breads were included as a reference. X-ray microtomography was applied to characterize the microstructure of the bread samples. For each sample type, oxygen diffusivity was calculated based on microstructural parameters. The samples for gas analyses were packaged under MA using vacuum compensation, using two vacuum strengths during the air evacuation step. The total porosity of all laboratory samples was above 75%, except for the side and bottom crusts which had a lower porosity (<70%). The porosities of the crumb and the side crust of the commercial bread were 80 and 76%, respectively. The connectivity density of the crumbs of the laboratory and commercial breads was 8 and 10 mm⁻³, respectively. The crust showed a larger resistance to oxygen diffusion than the crumb, but for both bread regions, the diffusivity was maximally ten times smaller than that of oxygen in air. When considering all data obtained from the gas analysis in the headspace immediately after packaging, oxygen levels of 0.1 ± 0.1% for strong vacuum and 3.8 ± 2.9% for weak vacuum were obtained, which differed significantly ($p < 0.05$). The results of the laboratory samples corresponded

well to those of industrially baked breads. It was concluded that vacuum strength during packaging determines gas transport in bread after packaging.

Keywords Bread · Microstructure · X-ray microtomography · Modified atmosphere packaging (MAP) · Gas exchange

Introduction

Bread is widely consumed all over the world. Unfortunately, the shelf life of bread is rather short due to staling processes and microbial spoilage. Staling processes are attributed to both physical and chemical changes occurring during storage, such as starch retrogradation, moisture migration and evaporation, and modification of the gluten structure (Gray and Bemiller 2003; Fadda et al. 2014). Those staling processes result in an important loss of sensorial quality, mainly caused by crumb firming and loss of freshness. However, crumb firming can be retarded by the use of specific additives in bread. Enzymes, such as amylases and xylanases, and emulsifiers, like hydroxypropyl methylcellulose and monoglycerides, reduce starch retrogradation, while moisture binders, such as hydrocolloids and fibers, improve moisture retention (Gray and Bemiller 2003; Bárcenas and Rosell 2005; Butt et al. 2008; Goesart et al. 2009; Fadda et al. 2014). Finally, the baking process, for instance the heating rate and the use of a baking pan, has an effect on the staling rate of bread (Purhagen et al. 2011; Fadda et al. 2014). Generally, the addition of well-selected additives and the optimization of the baking process delay staling processes. Consequently, microbial spoilage of bread is in most cases the main reason for a short shelf life. Since bread has a high water activity (a_w 0.96–0.98), almost all bacteria, yeasts, and molds are capable of growth (Jay et al.

✉ Sofie Morren
sofie.morren@kuleuven.be

¹ Faculty of Engineering Technology, Department of Microbial and Molecular Systems, Leuven Food Science and Nutrition Research Centre (LFoRCe), KU Leuven, Lab4Food, Kleinhofstraat 4, 2440 Geel, Belgium

² Department of Biosystems, BIOSYST-MeBioS, Division of Mechatronics, Biostatistics and Sensors, KU Leuven, Willem de Croylaan 42, 3001 Leuven, Belgium

2005; Needhama et al. 2005; Valerio et al. 2012). Nevertheless, spoilage by molds is the main factor limiting the shelf life of the bread. That is why methods to control mold growth are of significant importance to the bakery industry (Smith et al. 2004).

Molds are aerobic microorganisms, which implicates that elimination of oxygen from the packaging can extend the shelf life of the bread (Salminen et al. 1996). In addition, most molds are highly sensitive to carbon dioxide, which makes it very interesting to package the bread under modified atmosphere (MA) (Piergiovanni and Fava 1997; Smith et al. 2004). At carbon dioxide concentrations below 60%, residual oxygen ($\geq 1\%$) can promote mold growth. A complete elimination of oxygen from the packaging is however difficult, since air, and thus oxygen, can be trapped in the bread pores. Hence, gas exchange between the product and the headspace of the packaging is possible immediately after packaging (Piergiovanni and Fava 1997; Smith et al. 2004; Galić et al. 2009).

Bread has a highly porous texture with a porosity ranging between 72 and 84% of the total bread volume (Wang et al. 2011). This range indicates the wide diversity of bread microstructures that are available on the market. Many factors affect this variability, including the ingredients used and the bakery process applied (Cafarelli et al. 2014; Van Dyck et al. 2014). It is not known whether microstructure and/or packaging conditions influence gas exchange between bread and headspace during and immediately after packaging and whether or not the desired gas composition in the packaging is obtained. In this study, X-ray microtomography is combined with a gas diffusion model that directly incorporates the 3D microstructure of the bread. In order to monitor gas exchange between the bread and headspace, the gas composition is registered in function of time, both in the product and in the headspace of the packaging. Not only the residual oxygen level is recorded but also the actual carbon dioxide concentration. To investigate the effect of processing conditions, two packaging techniques are applied in order to compare the efficiency of both techniques.

Materials and Methods

Experimental Design

Tests were performed on breads prepared on laboratory scale and on breads produced in an industrial bakery. For the breads produced on laboratory scale, two variations on the bread-making process were used. The 3D microstructure of the two types of bread was analyzed using X-ray tomography. Based on the microstructural parameters, oxygen diffusivity in bread was calculated. In addition, gas exchange was also measured. This was done for fragments cut out of the breads as well as for whole breads. Fragments were cut from the crust

and the crumb for comparison. The cylindrical fragments were fixed into small PVC tubes and then packaged under modified atmosphere. Oxygen and carbon dioxide concentrations were monitored in the headspace as well as in the interior of the fragments to monitor gas exchange. As stated before, also breads produced at industrial scale, of the same type as the laboratory breads, were included in the study. Their 3D microstructure and the gas exchange in crumb and crust elements were determined for comparison to the laboratory breads.

Production of Breads at Laboratory Scale

Commercial, refined wheat flour (extraction rate 72%, as indicated by the supplier) was obtained from Bloemmolens Van Geel (Geel, Belgium). This flour was used for all breads baked. The flour had a protein content of 11.5 to 12.0%, a moisture content of 14.0 to 14.5%, and an ash content of 0.55 to 0.68% (product specifications obtained from supplier). A batch of dough consisted of 3000 g flour, 90 g instant yeast (Bruggeman, Gent, Belgium), 51 g NaCl, and 1740 g demineralized water. One batch of dough yielded 12 breads of about 400 g.

Two versions of a general bread-making procedure were followed. In particular, the number of punching steps, one (P1) or three (P3), was varied. Prior to the dough preparation, the temperature of the water was adjusted in order to obtain a dough temperature of 26 °C (Roussel and Chiron 2003). The yeast was suspended in the water, and the suspension was added to the dry ingredients. Then, all ingredients were mixed in a spiral mixer (type SM-25, Sinmag Europe BVBA, Zuienkerke, Belgium) for 3 min at 140 rpm and 5 min at 280 rpm. For P1, the dough was placed in a fermentation cabinet for 35 min at 25 °C and above 90% relative humidity (RH). At the end of the fermentation, the dough was divided into 12 parts of 400 g. Each part was punched for 2 min in a kitchen robot (type KMM020 Major Titanium, Kenwood, Mechelen, Belgium) at speed 1, molded, and placed in a baking mold (105 cm × 170 cm × 60 cm, type B0100, Clean Baking Products, Zwijndrecht, Belgium). Then, the dough was proofed for 50 min at 32 °C and above 90% RH in a fermentation cabinet (type Four 46.4 A/VAP Krystal, Bongard, Strasbourg, France). For P3, the dough was fermented (25 °C and above 90% RH) in the cabinet for 20 min after the mixing process. At the end of the first fermentation step, the dough was divided into 12 parts of 400 g. Each part was punched (2 min in the kitchen robot at speed 1) and subjected to a second fermentation step at 25 °C and above 90% RH for 15 min. Then, the parts were punched again (2 min at speed 1) and fermented at 32 °C and above 90% RH for 25 min. At the end of the fermentation, a final punching step (2 min at speed 1) was performed. After punching, the dough parts were molded, placed in the baking mold, and proofed for 25 min at 32 °C and above 90% RH.

Following proofing, the P1 and P3 dough was baked in an electric oven (type Four 46.4 A/VAP Krystal, Bongard, Strasbourg, France) for 40 min at a temperature starting at 240 °C and gradually being reduced to 200 °C. At the start of the baking process, 540 ml of water was vaporized in the baking chamber, as measured by the difference in the water volume in the reservoir for producing steam connected to the oven before and after the baking process by using a measuring cylinder. After baking, the breads were allowed to cool to ambient temperature for 2 h. The production of the different bread and element types was randomized over different production days. All bread-making conditions used in the laboratory were selected in consultation with industrial bakeries to be as close as possible to the industrial practice (except for the use of demi water). Processes involving 1 and 3 punching steps were chosen, as it was known from preliminary research (data not shown) that a wider range in microstructural parameters was obtained than when using 1 and 2 punching steps.

Industrially Produced Breads

Rectangular white breads of about 800 g were obtained from the industrial bakery Quintens Group NV (Diest, Belgium).

Microstructure Analysis

Cut cylindrical samples of crust and crumb were put in an airtight plastic sample holder of 22-mm diameter in order to prevent dehydration. The samples were scanned in a microCT scanner (Skyscan 1172, Bruker microCT, Kontich, Belgium) at X-ray source settings of 62 kV and 153 μ A. Projection images were taken at 0.30° steps over 180° rotation with a pixel resolution of 12.3 μ m. Scan time was between 23 and 24 min for each sample. Image reconstruction was performed with a standard back projection algorithm (NRecon software version 1.6.6, Bruker microCT, Kontich, Belgium). The resulting 3D image size was 1983 voxels \times 1983 voxels \times 750 voxels or 24 mm \times 24 mm \times 9 mm. The microstructure of both P1 and P3 breads was investigated on four positions, i.e., crumb, side crust, top crust, and bottom crust. For the industrially produced

breads, two positions were investigated, i.e., crumb and top crust. For each position, three samples taken from three loaves of three batches were scanned and analyzed.

3D image processing and morphological analysis of each sample was performed by CTAn software (version 1.12.0.0, Bruker microCT, Kontich, Belgium) and Avizo Fire 8.0 (VSG-FEI, Bordeaux, France). First, the bread sample was masked and then thresholding using an adaptive method (Bruker MicroCT, 2013) was performed to segment the solid matrix from the air spaces in the bread (Fig. 1). Morphological parameters of both the air and solid phases were calculated in CTAn and Avizo Fire. The structural parameters calculated were the following:

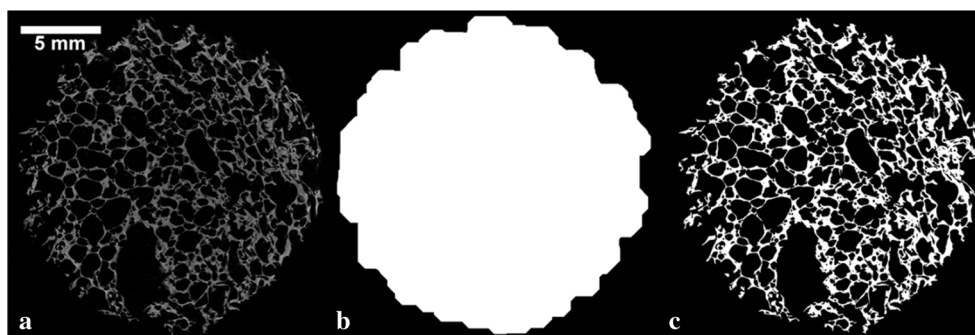
- The total porosity: the volume fraction of all air spaces in the sample volume
- The closed porosity: the volume fraction of isolated air spaces in the sample volume
- The number of isolated pores in the sample volume
- The number of connected pores in the sample volume after watershed segmentation of the open connected air space (Russ 2005; Herremans et al. 2013)
- The connectivity density of the microstructure: the degree to which parts of the air space are redundantly connected to each other (Gundersen et al. 1993)
- The structure thickness distribution of the bread matrix and pores: calculated by skeletonization of the matrix or air space volume, followed by a sphere fitting algorithm on each point of the skeleton (Hildebrand and Huesegger, 1997).

3D renderings of the microCT images were made in Avizo Fire 8.0 (FEI, Bordeaux, France).

Oxygen Diffusivity of Bread

Oxygen diffusion through the air space of the 3D microstructure of the bread samples was calculated using a pore network model (Ho et al. 2014). The binary image stacks were

Fig. 1 Micro-CT scan and image processing. **a** Gray scale slice of bread sample. **b** mask, **c** segmented image (adaptive threshold)



segmented further into individual pores and cell clusters by applying a watershed algorithm (Russ 2005). The final pore scale network consisted of a set of nodes, representing the individual pores, linked to their neighbors, determined by their connectivity. The coordinates of the centroids and the volume and area of the connections of individually labeled pores were determined and used in the computations of diffusion between nodes according to the equations presented in Ho et al. (2014) using the diffusivity of oxygen in air, $D_{O_2,air}$, equal to $176 \times 10^{-7} \text{ m}^2 \text{ s}^{-1}$. The system of equations of gas diffusion in the cell pore network was solved in Matlab (The Mathworks, Natick, MA, USA). At steady state, the total oxygen diffusion flux \mathbf{j} ($\text{mol m}^{-2} \text{ s}^{-1}$) entering and leaving the sample was determined by summing the mass flows entering the inlet nodes or leaving the outlet nodes and dividing by the total sample area. The apparent oxygen diffusivity D_{app} ($\text{m}^2 \text{ s}^{-1}$) was calculated from Fick's law of diffusion for the flux \mathbf{j} over a given concentration gradient ∇C across the sample ($\text{mol m}^{-3} \text{ m}^{-1}$):

$$D_{app} = -\frac{\mathbf{j}}{\nabla C}$$

Construction of Crumb and Crust Elements

Gas transport was studied in individual bread fragments. To investigate gas transport in one direction, the bread elements were fixed into PVC cylinders, thus preventing gas transport through the side face of the element. Cylindrical bread elements with a diameter of 50 mm and a height of 40 mm were prepared from the center of the bread, i.e., the crumb, and from three different bread surfaces, i.e., side crust, top crust, and bottom crust, using a hole saw with a diameter of 51 mm mounted on a drill (lowest speed, type PSB 850-2 RE, Robert Bosch GmbH, Stuttgart, Germany). These elements were fixed into PVC cylinders (outer diameter 5 cm, height 10 cm, thickness 2 mm) as illustrated in Fig. 2. At each end of the cylinder, one bread element was placed (for crust elements with the crust surface outwards). The border of the elements was glued to the cylinder (professional wood glue D2, Bison, Rotterdam, the Netherlands) to prevent gas transport between the bread element and the cylinder wall. A puncture was made in the center of the cylinder to serve as entrance point for the needle of the gas analyzer (Fig. 2). A septum (reusable type, diameter 15 mm, PBI Dansensor, Ringsted, Denmark) was fixed onto the puncture to create an air-tight seal.

Packaging of the Samples

Preformed bags (VAC090 PA/PE 20/70, thickness of 90 μm , Euralpack, Schoten, Belgium) were used in all packaging experiments. The size was 20 cm \times 30 cm for bread elements and 30 cm \times 40 cm for complete breads, to obtain a gas-to-product

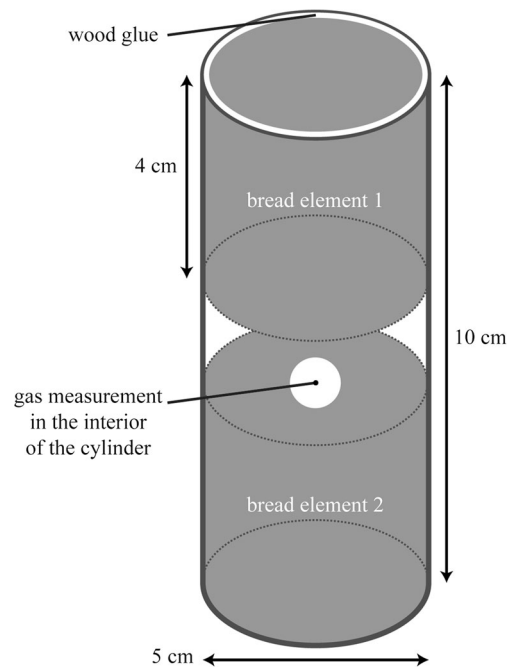


Fig. 2 Schematic representation of a PVC cylinder with two bread elements of a similar sample type of the same bread

ratio in the package of 2:1 for all experiments (Sivertsvik et al. 2004). The size of the commercial breads was 25 cm in length, 13 cm in width, and 12 cm in height (i.e., a volume of 3.9 l), the weight was 800 g and the package volume was about 7 l (in order to reach a substantial gas-to-product ratio which is the recommendation in modified atmosphere packaging (Sivertsvik et al. 2004; Arvanitoyannis 2012)). As indicated by the suppliers' technical information, the gas transmission rates of the bag were 50, 150, and 10 $\text{cm}^3/\text{m}^2 \text{ day atm}$ at 23 °C and 0% RH for oxygen, carbon dioxide, and nitrogen, respectively. The water vapor transmission rate was indicated to be 2.8 $\text{g}/\text{m}^2 \text{ day}$ at 23 °C and 85% RH. A gas mixture of 30% CO_2 and 70% N_2 (food grade, Praxair, Schoten, Belgium) was applied for all samples, since this is one of the most common gas mixtures used in the food industry and suitable for bread (personnel communication of gas supplier; Arvanitoyannis 2012). Packaging was performed using a vacuum sealer (C 200, Multivac, Mechelen, Belgium). Vacuum compensation was used to replace the air in the bags. Vacuum compensation comprised a first step in which air was evacuated from the package (and possibly the product) by creating an underpressure or vacuum and a second step in which the gas mixture is injected. Two different settings for the underpressure were used, further referred to as "strong vacuum" and "weak vacuum". The settings for the strong vacuum were 5 mbar for the bread elements and 20 mbar for the complete breads. For the weak vacuum condition, 150 mbar was used both for bread elements and complete breads. With the strong vacuum, the packaging conditions prevailing in a tray seal packaging machine were simulated, while with weak

vacuum, the conditions in a flow pack machine were simulated. Both machine types are frequently used in industrial bakeries. Gas injection was performed at 500 mbar for the bread elements and at 610 mbar for the complete breads. Six repetitions were included for every sample type. For the bread elements, each element was taken from another bread originating from another production batch. In the same way for the complete breads, for each repetition, a bread from another production batch was taken.

Gas Analysis of the Packaged Samples

After packaging, the gas composition in the headspace and in the product was determined using a portable gas analyzer (CheckPoint II O₂/CO₂, PBI Dansensor, Ringsted, Denmark). Oxygen and carbon dioxide concentrations in the headspace were measured at 1, 3, 5, 7, 9, 11, 30, and 60 min after packaging. Analyses in the product interior were carried out at 1, 7, 30, and 60 min after packaging. To measure the gas composition in the interior of the bread elements, the needle of the gas analyzer was inserted into the puncture of the cylinder (Fig. 2). To measure the gas composition in the interior of the complete breads, a septum (same type as described above) was placed directly on the crust in the center of the upper surface of the bread before packaging. Another septum was placed after packaging on the bag above the first. The needle was inserted for its full length (40 mm) through the two septa to reach the center of the bread.

Statistical Analysis

Statistical analyses were performed with IBM SPSS Statistics 19.0 (New York, USA). To detect significant differences, multiple analysis of variance (MANOVA) tests and post hoc Duncan tests were executed. In cases with fewer than three groups, an independent sample T test was carried out. Factors considered in the statistical analysis were the recipe (P1 or P3), the sample type (crumb, top crust, side crust, or bottom crust), the batch, and the sample number. Significance levels of 0.05 were applied.

Results and Discussion

Microstructure Analysis

Figure 3 presents 3D renderings of the microstructure of P1 and P3 breads (produced in the laboratory). The difference in cellular structure between top crust and crumb samples can be distinguished. The crust contained smaller pores in a thin layer near the surface of the bread, while the crumb contains larger pores throughout the bread matrix. Isolated small pores could

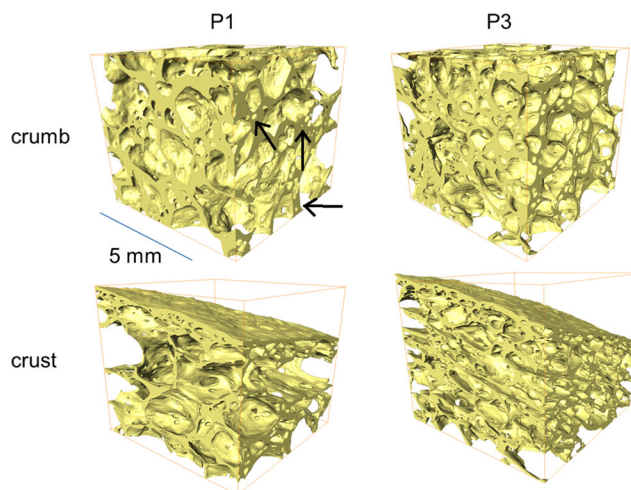


Fig. 3 3D renderings of bread samples of crumb and top crust for breads produced in the laboratory with one (P1) and three (P3) punching steps. Three connecting throats between pores are indicated with *black arrows*

be seen in the walls of the bread matrix. Increasing the number of punching steps reduced the size of the pores in both crumb and crust.

In Fig. 4, the structural parameters of the different breads produced in the laboratory are compared. The structure thickness is a measure for the average thickness of the bread matrix and the average diameter of the pores. The thickness of the bread walls was in the order of 0.1 to 0.2 mm, while the pores had sizes in the order of 1 mm diameter. The main effect is seen for P3 breads that had a reduced structure thickness of pores in the top crust. For the number of pores per bread volume, connected pores and isolated pores can be distinguished. Isolated pores are small pores present in the walls of the bread matrix. Connected pores are the large pores with a bread wall in between, but with small connecting throats (indicated with arrows on Fig. 3). There were two to four times more isolated pores than connected pores, but their volume was very small. The isolated pores represented less than 0.10% (closed porosity) of the bread volume for all breads. Because they are not part of the connected air space volume, the isolated pores will not play a significant role in gas transport during and after MA packaging. The connected pore density increased with increased punching (in a numerical way in the crumb and in a statistical way in the top crust), correlating with a decrease in pore volume. The total porosity was larger than 75%, did not vary much with punching, and was not different between crumb and top crust. Closed porosity was smaller in the crust. Hence, the volume of air in the walls of the bread matrix was smaller in the crust after baking as is evidenced by the values of matrix porosity expressing the volume of air per volume of bread matrix. The connectivity of the pores was large in all samples (more than seven connections per mm³, or more than eight connections per pore), varied considerable between samples and tended to be larger in the crust.

Fig. 4 Microstructure parameters of breads produced in the laboratory with one (P1) and three (P3) punching steps and for crumb (dark grey) and top crust (light grey) (*error bars* present standard deviations, $n = 3$). Structure thickness of the matrix (a) and of the pores (b), as well as the connected pore density (c), isolated pore density (d), the total porosity (e), the closed porosity (f), the connectivity density (g), and the matrix porosity (h) are shown

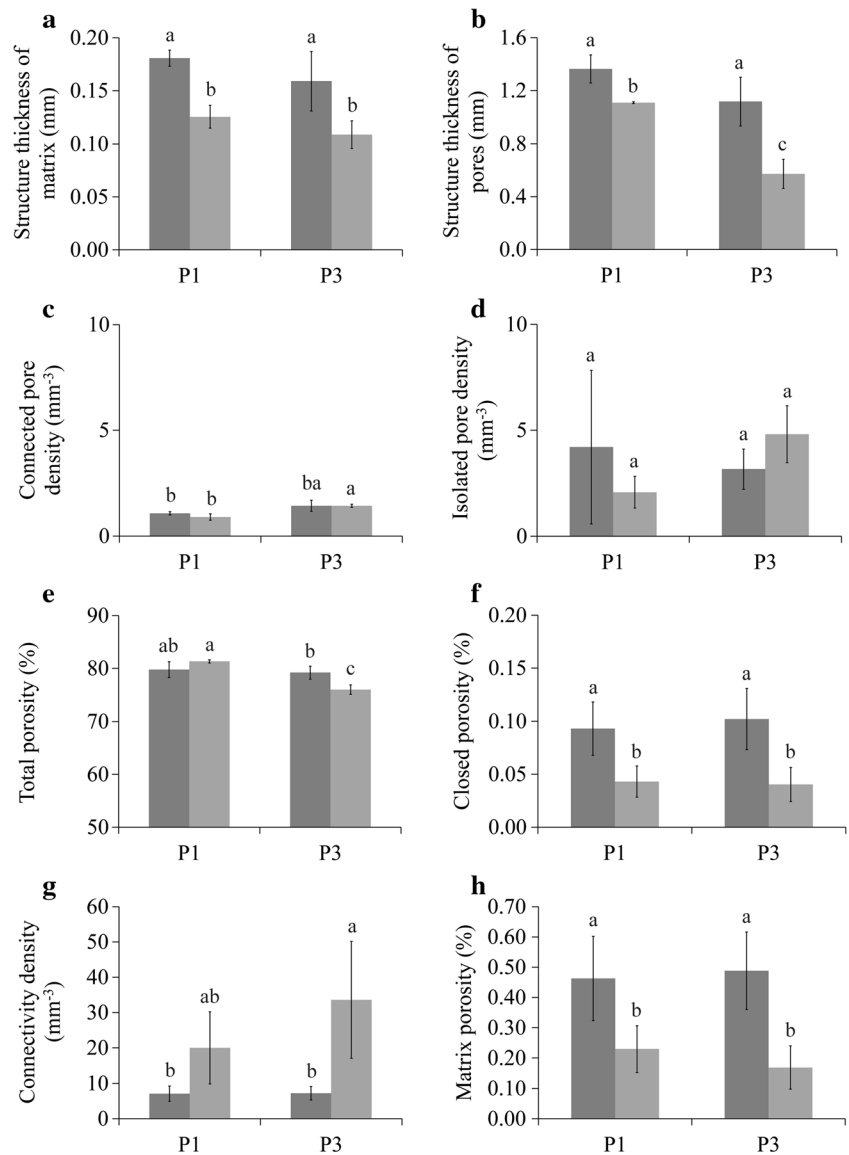


Figure 5 plots the structure thickness distribution of the pores in the laboratory bread samples, distinguishing crumb and top crust. Hardly any differences were observed for P1 breads, with the crust possessing a higher volume of pores smaller than 1-mm diameter. In P3 breads, however, there was a pronounced difference in pore-size distribution towards much smaller structure thickness of the pores in the crust,

which was also evidenced by the average structure thickness in Fig. 4.

Figure 6 shows the most important microstructure parameters of the different crusts of P3 bread (differences between crusts in P1 bread were similar, data not shown). All crusts had a similar pore thickness, but side and bottom crusts had a lower porosity (<70%). However, even though the bottom

Fig. 5 Structure thickness distribution of breads produced in the laboratory with one (a) and three (b) punching steps and for crumb (black line) and top crust (grey line) (*error bars* present standard deviations, $n = 3$)

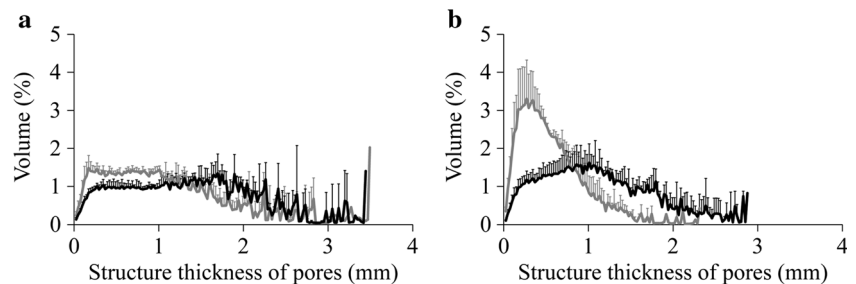
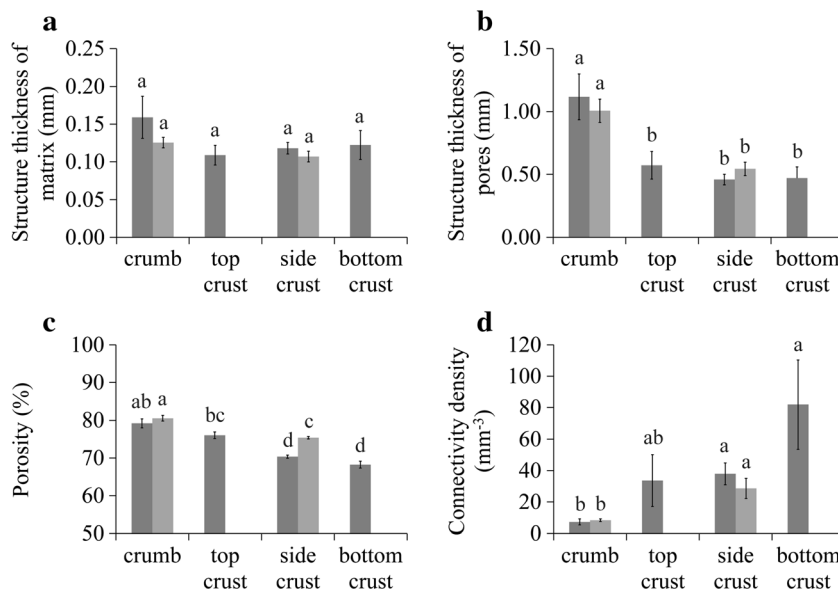


Fig. 6 Microstructure parameters of breads produced in the laboratory with three punching steps (dark grey square) and of commercial white bread (light grey). Structure parameters are given for crumb and crusts at different positions (*error bars* present standard deviations, $n = 3$). Structure thickness of the matrix (a) and of the pores (b), as well as the total porosity (c), and the connectivity density (d) are shown



crust had a more dense structure, the connectivity of the pores was very high. Figure 6 also presents the structure parameters of an industrially prepared white bread. In terms of the parameters considered, no substantial differences were found between laboratory and commercial breads, except for porosity of the crust which could be due to differences in the baking mold that was used.

Gas Diffusivity

Table 1 lists the apparent diffusivity values of the crumb and crust samples of the laboratory breads with different punching steps. Only significant differences were found in diffusivity of bottom crusts for different punching steps, the other parts were not different. Variability is considerable, and the diffusivity is relatively large: the crumb values are only three to four times smaller than that of oxygen in air, the crust are five to ten times smaller. This is not unexpected due to the high porosity and very well connected air spaces in the bread (Figs. 4 and 6). Crust diffusivity is smaller than crumb diffusivity in P3 breads only, conferring with the observations of lower porosity

(Fig. 4) and differences in the structure thickness distributions (Fig. 5). The crust of P3 breads had narrower throats where the gas has to channel through, which appears to be the limiting factor for diffusion (Ho et al. 2014). The differences are, however, insignificant and diffusion in the breads is not limited to the same extent as observed in other foods such as fruit, in which the porosity is low and pore sizes are in the micrometer range (Ho et al. 2010a, b; Ho et al. 2011; Warning et al. 2014).

The oxygen diffusivity of industrially baked breads corresponds well to that of the laboratory samples (Table 1), as do the structure parameters (Fig. 6). The crust exhibits a larger resistance to oxygen diffusion than the crumb, but for both bread regions, the diffusivity is relatively large and maximally ten times smaller than that of oxygen in air.

Gas Exchanges Between Product and Headspace

When packaging food under MA, the quality of the packaging process can be evaluated in the first place by comparing the gas composition obtained in the headspace

Table 1 Apparent oxygen diffusivity D_{app} ($\times 10^{-7} \text{ m}^2 \text{ s}^{-1}$) of breads prepared on laboratory scale with one (P1) or three (P3) punching steps and of industrially produced breads (\pm standard deviation, $n = 3$)

	Crumb	Side crust	Top crust	Bottom crust
Breads prepared on laboratory scale				
P1	47.9 ± 5.9 Aa	34.3 ± 6.7 ABa	28.0 ± 20.3 ABa	21.2 ± 1.7 Bb
P3	38.7 ± 5.5 Aa	27.3 ± 2.7 Aa	15.4 ± 8.1 Aa	33.9 ± 2.7 Aa
Breads produced in an industrial bakery				
	44.0 ± 7.6 Aa	–	18.8 ± 5.3 Ba	–

Uppercase letters represent comparison along horizontal axis while lowercase letters represent comparison along vertical axis

immediately after packaging to the composition of the gas mixture used, i.e., the desired gas composition (30% CO₂ and 70% N₂ in this study). When considering all data obtained for bread elements and complete breads produced in the laboratory (Figs. 7, 8, and 9), on average oxygen levels of $0.1 \pm 0.1\%$ for strong vacuum and $3.8 \pm 2.9\%$ for weak vacuum were observed in the headspace immediately after packaging. Similarly, the average carbon dioxide concentration immediately after packaging was $30.5 \pm 1.5\%$ and $24.7 \pm 5.5\%$ for strong and weak vacuum, respectively. Both for oxygen and carbon dioxide, the values for strong vacuum (Fig. 7) differed in a statistically significant way from those for weak vacuum (Fig. 8) ($p < 0.05$). The data indicate that when using strong vacuum during packaging (which can be obtained in a tray seal machine), the gas composition reached in the headspace immediately after packaging is equal to that of the mixture used. When packaging using weak vacuum (as in a flow pack machine), there is a substantial deviation in the headspace from the desired composition. This is especially crucial for oxygen, as the residual oxygen level after packaging has a major influence on the shelf life of bread. Other studies on packaging of bread and bakery products report residual oxygen levels between those obtained here for strong and weak vacuum. Degirmencioglu et al. (2011) and Rasmussen and Hansen (2001) found residual oxygen levels of less than 1% when using 100% carbon dioxide or 100% nitrogen, or mixtures of both gasses, for packaging. In these studies, however, the packaging technique and/or parameters were not stated. For headspace carbon dioxide concentrations immediately after packaging, no data were found in

literature, although this parameter is also important for shelf life.

In addition to the gas composition obtained immediately after packaging, its evolution during storage is considered. The comparison of the profiles measured in the headspace and inside the product illustrates the gas transport between those two compartments. In Fig. 7, the gas profiles obtained for different volume elements of breads, produced at laboratory scale with one or three punching steps, and then packaged using strong vacuum are depicted. Two types of bread elements were studied, i.e., crumb and side crust elements. The oxygen concentration reached 60 min after packaging did not differ significantly from the initial value, except for the side crust obtained with three punching steps ($p = 0.006$). The latter is probably due to an invisible leakage in the package seal, because the oxygen concentration in the product increased slightly after 60 min. Generally, there was no or little exchange of oxygen between headspace and product. In contrast, although not very visible on the figure, for carbon dioxide gas exchange between product and headspace was recorded. In all cases, the concentration measured at 60 min after packaging differed significantly ($p < 0.05$) from initial concentrations, except in the headspace for the crumb (both one and three punching steps).

For laboratory bread elements packaged using weak vacuum, four types of bread elements were investigated, i.e., crumb, side crust, top crust, and bottom crust elements. The gas profiles recorded are shown in Fig. 8. All samples packaged under weak vacuum showed clear gas exchanges. In the headspace, the oxygen concentration increased whereas the carbon dioxide concentration

Fig. 7 Gas profiles of bread elements of white rectangular breads produced at laboratory scale, packaged under modified atmosphere using strong vacuum (error bars present standard deviations, $n = 6$). Results of the crumb element in the headspace (a) and the product (b), and the side crust in the headspace (c) and the product (d) are shown. Legend of the markers: *black triangle* oxygen concentration of one-time punching (P1), *white triangle* carbon dioxide concentration of P1, *black circle* oxygen concentration of three-time punching (P3), *white circle* carbon dioxide concentration of P3

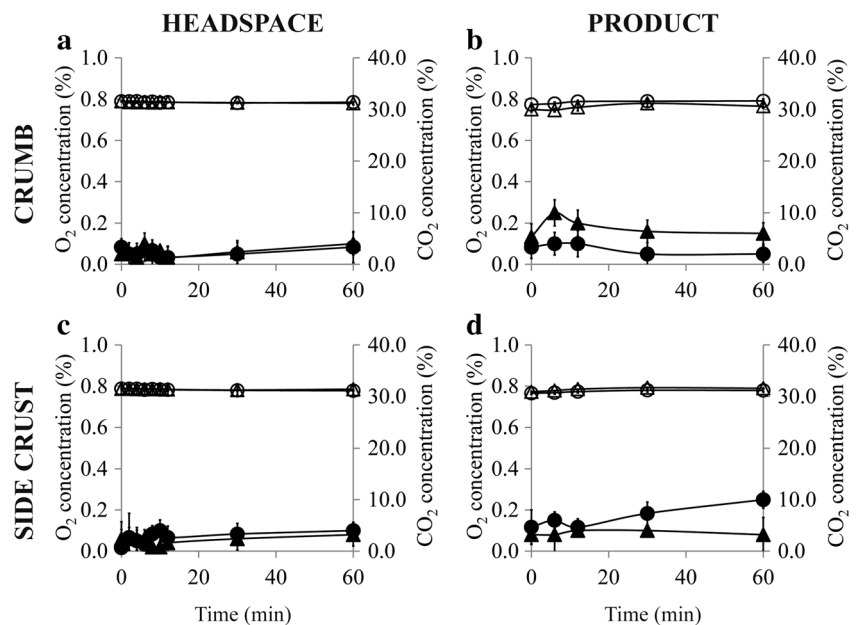
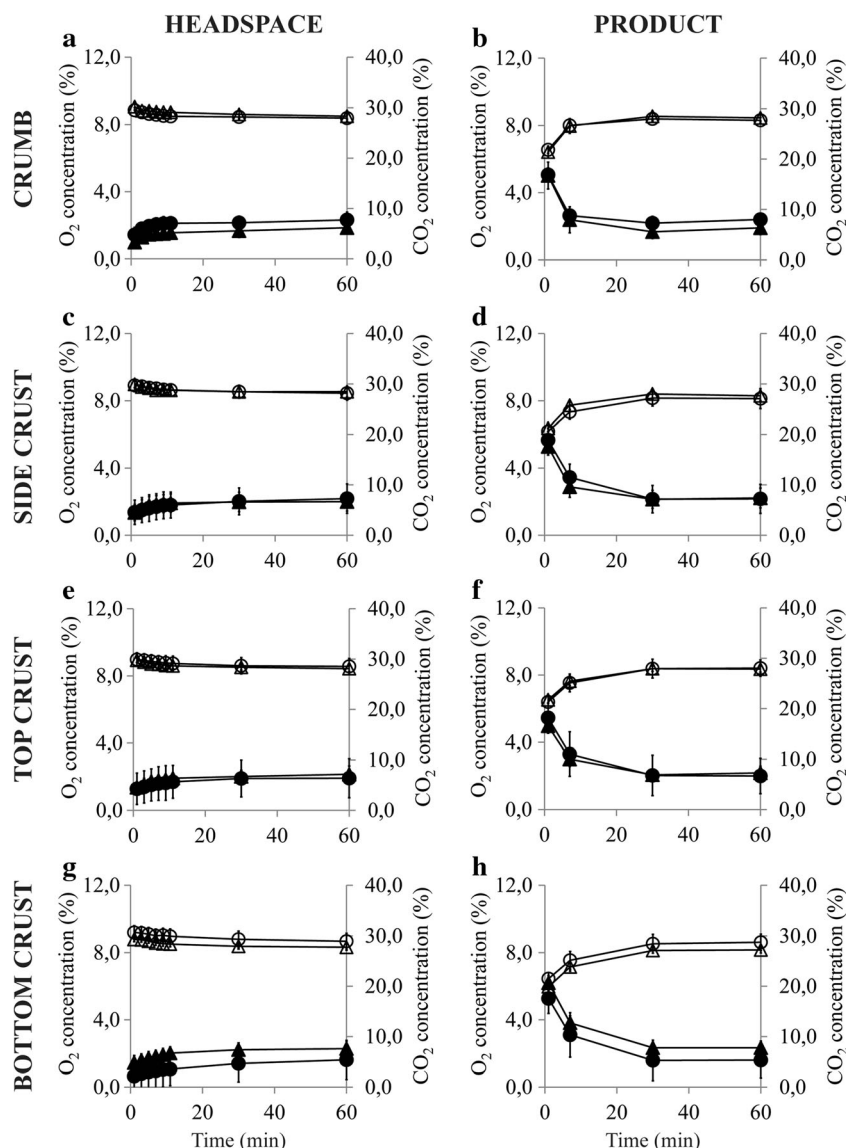


Fig. 8 Gas profiles of bread elements of white rectangular breads produced at laboratory scale, packaged under modified atmosphere using weak vacuum (*error bars* present standard deviations, $n = 6$). Results of the crumb element in the headspace (a) and the product (b), side crust in the headspace (c) and the product (d), top crust in the headspace (e) and the product (f), and the bottom crust in the headspace (g) and the product (h) are shown. Legend of the markers: *black triangle* oxygen concentration of one-time punching (P1), *white triangle* carbon dioxide concentration of P1, *black circle* oxygen concentration of three-time punching (P3), *white circle* carbon dioxide concentration of P3



decreased. The opposite effect was observed in the product. The effect was more pronounced in the product than in the headspace, obviously because initial values differed more from the values at steady state than for the headspace. Table 2 illustrates the influence of the type of bread element (crumb, side crust, top crust, and bottom crust) and the influence of the production process (one or three punching steps, P1 and P3, and hence product microstructure) on the gas composition obtained immediately after packaging using weak vacuum. In Table 2, a p value below 0.05 indicates that the type of bread element or the type of production process has a significant influence on the initial oxygen or carbon dioxide concentration in the headspace or in the product. The type of bread element showed a significant influence both on the initial oxygen and carbon dioxide concentrations for P1, but not for P3 (except in the product). The production process (P1 or P3)

showed no significant influence on the initial oxygen and carbon dioxide values, except in the headspace as well as in the product for the bottom crust element. In the latter case, the residual oxygen level in the headspace of the bottom crust obtained by P3 was lower than the residual oxygen level of the bottom crust obtained by P1. In other words, the gas composition reached after packaging of the bottom crust obtained by three punching steps was closer to the gas mixture used for packaging than for the bottom crust obtained by punching once. This indicates that the bottom crust obtained by three punching steps is more permeable for gasses than the one obtained by punching once, which corresponds to the values for apparent oxygen diffusivity in Table 1.

Figure 9 shows the gas profiles of complete white breads produced at laboratory scale. The initial oxygen concentration of complete breads packaged using strong vacuum (Fig. 9a, b)

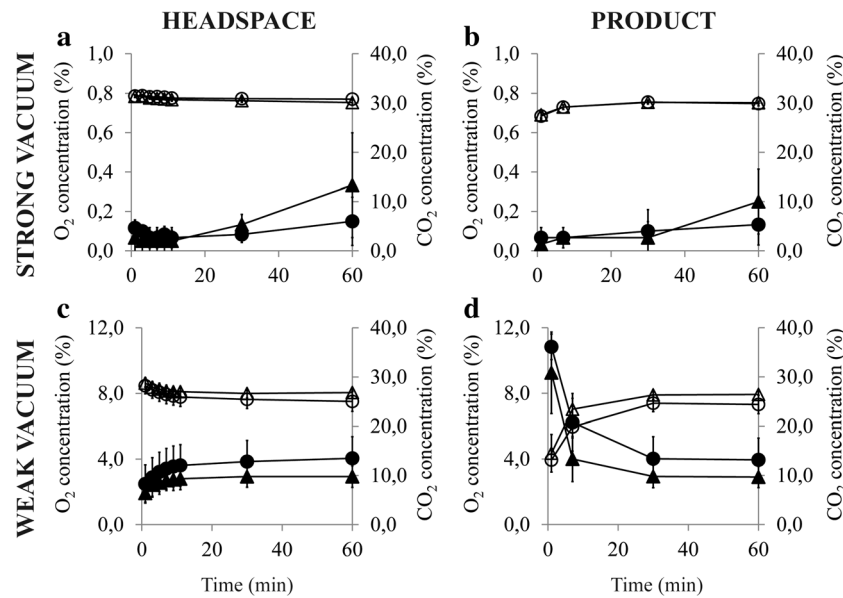


Fig. 9 Gas profiles of complete white rectangular breads produced at laboratory scale, packaged under modified atmosphere (error bars present standard deviations, $n = 6$). Results of the breads packaged under strong vacuum, measurement in the headspace (a) and the product (b), and results of the breads packaged under weak vacuum,

measurement in the headspace (c) and the product (d), are shown. Legend of the markers: *black triangle* oxygen concentration of one-time punching (P1), *white triangle* carbon dioxide concentration of P1, *black circle* oxygen concentration of three-time punching (P3), *white circle* carbon dioxide concentration of P3

did not differ significantly ($p > 0.05$) from that observed after 60 min. In contrast, the values for carbon dioxide concentration measured immediately after packaging differed significantly ($p = 0.000$) from those measured 60 min later, pointing towards a substantial gas exchange. The initial oxygen and carbon dioxide concentrations of complete breads packaged

using weak vacuum (Fig. 9c, d) differed significantly from the concentrations observed at 1 h of storage, especially in the product ($p = 0.000$). In the product, a clear decrease of the oxygen concentration was recorded, whereas the carbon dioxide concentration increased. The opposite trend, although less pronounced, was found in the headspace. When the two production processes, P1 and P3, are compared to each other for complete breads, it can be seen that the initial oxygen and carbon dioxide concentrations did not differ significantly, nor for strong or weak vacuum.

Table 2 Influence of the type of bread element (crumb, side crust, top crust, or bottom crust) and recipe (one-punching step, P1, or three-punching steps, P3) on the initial gas composition (oxygen and carbon dioxide concentration) when packaging using weak vacuum (based on the data shown in Fig. 8), as represented by the p value

Factor	Location of measurement	Variable	Oxygen p value	Carbon dioxide p value
Type of bread element	Headspace	P1	0.008	0.001
		P3	0.081	0.123
	Product	P1	0.009	0.016
		P3	0.237	0.015
Type of production process	Headspace	Crumb	0.199	0.324
		Side crust	0.996	0.956
		Top crust	0.384	0.749
		Bottom crust	0.009	0.002
	Product	Crumb	0.453	0.735
		Side crust	0.556	0.120
		Top crust	0.593	0.107
		Bottom crust	0.032	0.034

The data obtained for the bread elements (Figs. 7 and 8) can also be compared to those obtained for the complete breads (Fig. 9). When elements or complete breads were packaged using strong vacuum, little, or no gas exchange between product and headspace were found in both cases. However, when weak vacuum was applied, a clear exchange between headspace and product were recorded for elements as well as for complete breads. For the elements, as measured in the product, the average initial oxygen level was $5.3 \pm 0.7\%$ (mean of P1 and P3). For the complete products, the corresponding value was $10.0 \pm 1.9\%$, which was significantly higher than that of the elements ($p = 0.000$). For carbon dioxide measured in the product, the average initial values (mean of P1 and P3) in the elements was $21.3 \pm 1.2\%$ and for the complete breads, it was $13.8 \pm 2.8\%$, which was also a significant difference ($p = 0.000$). Similar ratios between oxygen and carbon dioxide values between elements and complete breads were found after 60 min of storage. Therefore, it can be concluded that similar gas exchange prevailed in

the elements as in the breads, and hence, the elements were representative for complete breads. The values in the elements being closer to the desired gas composition than those in the breads can be explained by the fact that the volume of the complete breads was larger than that of the elements, implicating a larger distance and time for gas transport.

Industrial Relevance

The diffusion of oxygen from the bread into the headspace of a MA package takes maximally 30 min due to the oxygen diffusion limitation of the bread crumb and crust. That was demonstrated on small samples as well as on intact breads. Industrial relevance was also confirmed by the data obtained from the elements from industrially produced breads packaged under modified atmosphere (Fig. 10). Figure 10 (commercial bread elements) can be compared to the crumb and side crust data in Fig. 8 (laboratory bread elements), as the same packaging conditions, and in particular a weak vacuum, were applied. The gas evolution profiles are highly similar for the commercial and the laboratory samples, both in the headspace as in the product, even though the laboratory and the commercial breads were not produced using the same ingredients. Summarized over the whole study, not the ingredients used or the production process (see earlier, P1 vs. P3), but rather the position in the bread (as indicated by the different element types) and the applied vacuum strength have an influence on gas transport in bread.

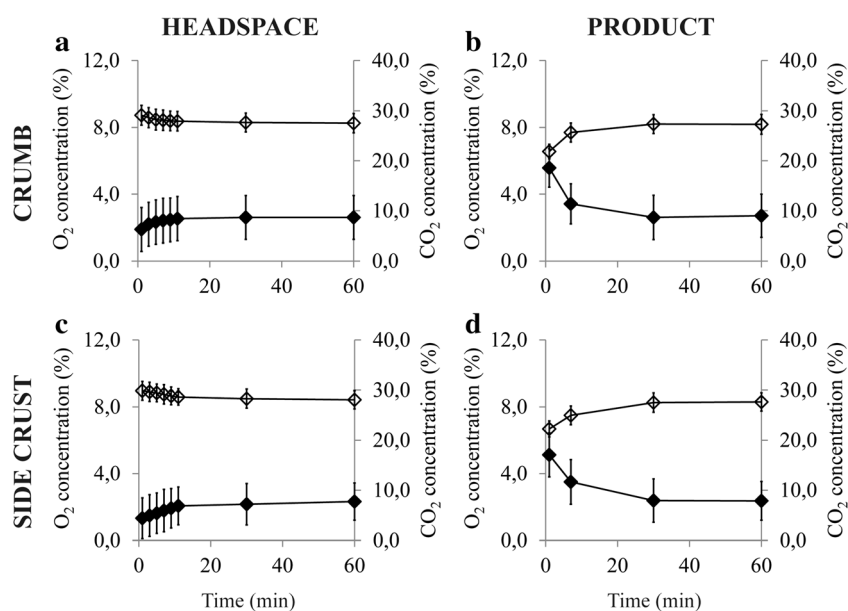
To verify the MA packaging process, it is thus recommended to wait for at least 30 min to verify the gas concentration in the headspace. Although limited, diffusion clearly plays a role

after weak vacuum packaging, operators do not need to adapt the process for every bread type as responses are expected to be rather similar. A plausible explanation is the fact that the majority of the pores in the bread structure is open and connected to the outside atmosphere. For example, we observed that smaller pore sizes in the bread crust were accompanied with a higher degree of connectivity. Therefore, the crust did not act as an additional barrier for gas exchange, as is often expected. The crust microstructure allowed an easy and relatively rapid passage of gas during and after packaging using vacuum compensation.

Conclusions

The objective of this study was to examine bread microstructure, oxygen diffusion properties, and gas exchanges between bread and headspace after packaging in modified atmosphere (MA). Microstructure did not influence oxygen diffusion in laboratory as well as in the industrially prepared bread to a significant extent. In addition, the bread crust did not act as a barrier for oxygen diffusion. On the other hand, industrial bakeries should know that vacuum compensation is preferred above flushing to obtain good gas conditions in the package, as was demonstrated in our work. A vacuum strength as high as possible (according to the packaging equipment available and according to the maximum strength the product can withstand) should be used. A high vacuum strength during the air evacuation step favors gas exchange, not only in the headspace but also within the product. It can also be speculated that the bread volume as well as its geometry play a role in both gas transport and concentrations obtained in

Fig. 10 Gas profiles of bread elements of industrially produced white rectangular breads, packaged under modified atmosphere using weak vacuum (error bars present standard deviations, $n = 6$). Results of the crumb element in the headspace (a) and the product (b), and the side crust in the headspace (c) and the product (d) are shown. Legend of the markers: *black diamond* oxygen concentration, *white diamond* carbon dioxide concentration



steady state in product and headspace. Further research is needed to elucidate this.

Acknowledgements Financial support was obtained for this work from the CORNET-project “Bake.IMPACT: Innovations in Mild decontamination and PACKaging Technologies for bakery products” (IWT-120276, VLAIO, Vlaams Agentschap Ondernemen & Innoveren, Brussels, Belgium).

References

- Arvanitoyannis, I. S. (2012). Principles of MAP and definitions of MAP, CA and AP. In I. S. Arvanitoyannis & D.-W. Sun (Eds.), *Modified atmosphere and active packaging technologies*. Boca Raton: CRC Press.
- Bárceñas, M. E., & Rosell, C. M. (2005). Effect of HPMC addition on the microstructure, quality and aging of wheat bread. *Food Hydrocolloids*, *19*, 1037–1043.
- Bruker MicroCT. (2013). CT-analyser version 1.13: The user’s guide. <http://www.skyscan.be/products/downloads.htm>. Accessed 8 May 2015.
- Butt, M. S., Tahir-Nadeem, M., Ahmad, Z., & Sultan, M. T. (2008). Xylanases and their applications in baking industry. *Food Technology and Biotechnology*, *46*(1), 22–31.
- Cafarelli, B., Spada, A., Laverse, J., Lampignano, V., & Del Nobile, M. A. (2014). X-ray microtomography and statistical analysis: tools to quantitatively classify bread microstructure. *Journal of Food Engineering*, *124*, 64–71.
- Degirmencioglu, N., Göcmen, D., Inkayan, A. N., Aydin, E., Guldaz, M., & Genec, S. (2011). Influence of modified atmosphere packaging and potassium sorbate on microbiological characteristics of sliced bread. *Journal of Food Science and Technology*, *48*(2), 236–241.
- Fadda, C., Sanguinetti, A. M., Del Caro, A., Collar, C., & Piga, A. (2014). Bread staling: updating the view. *Comprehensive Reviews in Food Science and Food Safety*, *13*, 473–492.
- Galić, K., Čurić, D., & Gabrić, D. (2009). Shelf life of packaged bakery goods: a review. *Critical Reviews in Food Science and Nutrition*, *49*, 405–426.
- Goesaert, H., Slade, L., Levine, H., & Delcour, J. A. (2009). Amylases and bread firming: an integrated view. *Journal of Cereal Science*, *50*, 345–352.
- Gray, J. A., & Bemiller, J. N. (2003). Bread staling: molecular basis and control. *Comprehensive Reviews in Food Science and Food Safety*, *2*, 1–21.
- Gundersen, H. J. G., Boyce, R. W., Nyengaard, J. R., & Odgaard, A. (1993). The Conneuler: unbiased estimation of connectivity using physical disectors under projection. *Bone*, *14*, 217–222.
- Herremans, E., Bongaers, E., Estrade, P., Gondek, E., Hertog, M., Jakubczyk, E., Nguyen, N., Rizzolo, A., Saeys, W., Spinelli, L., Torricelli, A., Vanoli, M., Verboven, P., & Nicolai, B. (2013). Microstructure-texture relationships of aerated sugar gels: novel measurement techniques for analysis and control. *Innovative Food Science & Emerging Technologies*, *18*, 202–211.
- Hildebrand, T., & Huegsegger, P. (1997). A new method for the model independent assessment of thickness in three dimensional images. *Journal of Microscopy*, *185*, 67–75.
- Ho, Q., Verboven, P., Fanta, S., Abera, M., Retta, M., Herremans, E., Defraeye, T., & Nicolai, B. (2014). A multiphase pore scale network model of gas exchange in apple fruit. *Food and Bioprocess Technology*, *7*, 482–495.
- Ho, Q. T., Verboven, P., Verlinden, B. E., Herremans, E., Wevers, M., Carmeliet, J., & Nicolai, B. M. (2011). A three dimensional multiscale model for gas exchange in fruit. *Plant Physiology*, *155*, 1158–1168.
- Ho, Q. T., Verboven, P., Verlinden, B. E., Schenk, A., Delele, M. A., Rolletschek, H., Vercammen, J., & Nicolai, B. M. (2010a). Genotype effects on internal gas gradients in apple fruit. *Journal of Experimental Botany*, *61*, 2745–2755.
- Ho, Q. T., Verboven, P., Verlinden, B. E., & Nicolai, B. M. (2010b). A model for gas transport in pear fruit at multiple scales. *Journal of Experimental Botany*, *61*, 2071–2081.
- Jay, J. M., Loessner, M. J., & Golden, D. A. (2005). *Modern food microbiology*. New York: Springer Science + Business Media.
- Needhama, R., Williams, J., Beales, N., Voysey, P., & Magan, N. (2005). Early detection and differentiation of spoilage of bakery products. *Sensors and Actuators B*, *106*, 20–23.
- Piergiovanni, L., & Fava, P. (1997). Minimizing the residual oxygen in modified atmosphere packaging of bakery products. *Food Additives and Contaminants*, *14*, 765–773.
- Purhagen, J. K., Sjöö, M. E., & Eliasson, A.-C. (2011). Starch affecting anti-staling agents and their function in freestanding and pan-baked bread. *Food Hydrocolloids*, *25*, 1656–1666.
- Rasmussen, P. H., & Hansen, Å. (2001). Staling of wheat bread stored in modified atmosphere. *Lebensmittel-Wissenschaft und Technologie*, *34*, 487–491.
- Roussel, P., & Chiron, H. (2003). *Les pains français: Évolution, qualité, production*. Vesoul: Maé-Erti.
- Russ, J. C. (2005). *Image analysis of food microstructure*. Boca Raton: CRC Press LLC.
- Salminen, A., Latva-Kala, K., Randell, K., Hurme, E., Linko, P., & Ahvenianen, R. (1996). The effect of ethanol and oxygen absorption on the shelf-life of packed sliced rye bread. *Packaging Technology and Science*, *9*, 29–42.
- Sivertsvik, M., Jeksrud, W. K., Vagane, A., & Rosnes, J. T. (2004). Solubility and adsorption rate of carbon dioxide into non-respiring foods. Part 1: development and validation of 396 experimental apparatus using a manometric method. *Journal of Food Engineering*, *61*, 449–458.
- Smith, J. P., Daifas, D. P., El-Khoury, W., Koukoutsis, J., & El-Khoury, A. (2004). Shelf life and safety concerns of bakery products: a review. *Critical Reviews in Food Science and Nutrition*, *44*, 19–55.
- Valerio, F., De Bellis, P., Di Biase, M., Lonigro, S. L., Giussani, B., Visconti, A., Lavermicocca, P., & Sisto, A. (2012). Diversity of spore-forming bacteria and identification of *Bacillus amyloliquefaciens* as a species frequently associated with the ropy spoilage of bread. *International Journal of Food Microbiology*, *156*, 278–285.
- Van Dyck, T., Verboven, P., Herremans, E., Defraeye, T., Van Campenhout, L., Wevers, M., Claes, J., & Nicolai, B. (2014). Characterisation of structural patterns in bread as evaluated by X-ray computer tomography. *Journal of Food Engineering*, *123*, 67–77.
- Wang, S., Austin, P., & Bell, S. (2011). It’s a maze: the pore structure of bread crumbs. *Journal of Cereal Science*, *54*, 203–210.
- Warning, A., Verboven, P., Nicolai, B., van Dalen, G., & Datta, A. K. (2014). Computation of mass transport properties of apple and rice from X-ray microtomography images. *Innovative Food Science & Emerging Technologies*, *24*, 14–27.